EBioMedicine 36 (2018) 209–220

Contents lists available at ScienceDirect

EBioMedicine

journal homepage: www.ebiomedicine.com

EBioMedicine
Published by THE LANCET

Research paper

Cancer-associated fibroblasts contribute to oral cancer cells proliferation and metastasis via exosome-mediated paracrine miR-34a-5p

Yao-yin Li [a,b,*], Yi-wei Tao [b,c], Gao Shuo [a], Li Pei [a], Jian-mao Zheng [c], Si-en Zhang [d], Jianfeng Liang [d], Zhang Yuejiao [c]

[a] Department of Pediatric Dentistry, Guanghua School of Stomatology, Hospital of Stomatology, Sun Yat-sen University, Guangzhou, Guangdong 510055, China
[b] Guangdong Province Key Laboratory of Stomatology, Guangzhou, Guangdong 510080, China
[c] Department of Operative Dentistry and Endodontics, Guanghua School of Stomatology, Hospital of Stomatology, Sun Yat-sen University, Guangzhou, Guangdong 510055, China
[d] Department of Oral and Maxillofacial Surgery, Guanghua School of Stomatology, Hospital of Stomatology, Sun Yat-sen University, Guangzhou, Guangdong 510055, China

ARTICLE INFO

Article history:
Received 5 July 2018
Received in revised form 20 August 2018
Accepted 5 September 2018
Available online 20 September 2018

Keywords:
Oral squamous cell carcinoma
CAFs
Exosomes
miR-34a-5p
AXL

ABSTRACT

Background: Cancer-associated fibroblasts (CAFs) play an important role in regulating tumor progression by transferring exosomes to neighboring cells. Our aim was to clarify the role of microRNA encapsulated in the exosomes derived from CAFs in oral squamous cell carcinoma (OSCC).
Methods: We examined the microRNA expression profiles of exosomes derived from CAFs and donor-matched normal fibroblasts (NFs) from patients with OSCC. We used confocal microscopy to examine the transportation of exosomal miR-34a-5p between CAFs and OSCC cells. Next, luciferase reporter and its mutant plasmids were used to confirm direct target gene of miR-34a-5p. Phenotypic assays and in vivo tumor growth experiments were used to investigate the functional significance of exosomal miR-34a-5p.
Findings: We found that the expression of miR-34a-5p in CAF-derived exosomes was significantly reduced, and fibroblasts could transfer exosomal miR-34a-5p to OSCC cells. In xenograft experiments, miR-34a-5p overexpression in CAFs could inhibit the tumorigenesis of OSCC cells. We further revealed that miR-34a-5p binds to its direct downstream target *AXL* to suppress OSCC cell proliferation and metastasis. Stable ectopic expression of *AXL* in OSCC cells overexpressing miR-34a-5p restored proliferation and motility abolished by the miRNA. The miR-34a-5p/AXL axis promoted OSCC progression via the AKT/GSK-3β/β-catenin signaling pathway, which could induce the epithelial-mesenchymal transition (EMT) to promote cancer cells metastasis. The miR-34a-5p/AXL axis enhanced nuclear translocation of β-catenin and then induced transcriptional upregulation of *SNAIL*, which in turn activated both MMP-2 and MMP-9.
Interpretation: The miR-34a-5p/AXL axis confers aggressiveness in oral cancer cells through the AKT/GSK-3β/β-catenin/Snail signaling cascade and might represent a therapeutic target for OSCC.
Fund: National Natural Science Foundation of China.

1. Introduction

Oral squamous cell carcinoma (OSCC) is one of the leading causes of cancer death worldwide, and nearly 50% of patients die from the disease [1]. Regardless of the therapeutic approach, location, or stage of the disease, >50% of patients experience a relapse [2]. Cell interactions within the tumor microenvironment are now recognized as a crucial element in tumor progression [3]. As the second most numerous cell type in the oral mucosa, fibroblasts represent a dynamic population of cells that show functional and phenotypic diversity. Among the various fibroblastic phenotypes, activated fibroblasts are the most important group, and are characterized by the expression of α-smooth muscle actin (α-SMA) and fibroblast activation protein (FAP) [4]. Activated fibroblasts that are found in association with cancer cells are known as cancer-associated fibroblasts (CAFs) [4]. CAFs are found in almost all solid tumor tissues and play an important role in the malignant progression of cancer, including epithelial-to-mesenchymal transition (EMT) and metastasis [5]. Therefore, CAFs are thought to be "the dark side of the coin" in tumorigenesis [6].

Abbreviations: OSCC, oral squamous cell carcinoma; CAF, cancer-associated fibroblast; NF, normal fibroblast; ECM, extracellular matrix; TEM, transmission electron microscopy; MMP, matrix metalloproteinase; MT1-MMP, membrane-type 1 matrix metalloproteinase; SMA, smooth muscle actin; FAP, fibroblast activation protein; TGF, transforming growth factor; miRNA, microRNA; EMT, Epithelial-Mesenchymal Transition.

* Corresponding author at: Department of Pediatric Dentistry, Guanghua School of Stomatology, Hospital of Stomatology, Sun Yat-sen University, Guangzhou, Guangdong 510055, China.
E-mail address: liyaoyin@mail.sysu.edu.cn (Y. Li).

https://doi.org/10.1016/j.ebiom.2018.09.006

Research in Context

Cancer-associated fibroblasts (CAFs) play an important role in tumor progression by secreting exosomes. Here, we performed microRNA (miRNA) sequencing of exosomes derived from CAFs and donor-matched normal fibroblasts (NFs) from patients with oral squamous cell carcinoma (OSCC). MiR-34a-5p levels were downregulated in CAF-derived exosomes, and CAFs could transfer exosomal miR-34a-5p to OSCC cells. Moreover, miR-34a-5p binds to its direct downstream target *AXL* to suppress OSCC cell proliferation and metastasis. The miR-34a-5p/AXL axis induced epithelial-mesenchymal transition (EMT) and promoted OSCC progression via the AKT/GSK-3β/β-catenin/Snail signaling cascade. MiR-34a-5p/AXL axis represent a promising therapeutic target to treat OSCC.

CAFs play a role in tumor development via cell-cell interaction or cross-talk with tumor cells by secreting growth factors, cytokines, and exosomes [7]. Many studies have shown that fibroblasts in the tumor microenvironment can "communicate" with tumor cells via exosomes [8]. Exosomes are nanovesicles with a diameter ranging from 40 to 120 nm. In addition to their size, exosomes can be identified by virtue of their unique proteins, including Rab GTPases, integrins, Alix (ALG-2-interacting protein X), TSG101 (tumor susceptibility gene 101), and tetraspanins (CD63, CD9, CD81, and CD82) [9]. Exosomes are derived from endocytic compartments and contain mRNAs, proteins, DNA, and microRNAs (miRNAs) [10]. They may induce signal transduction or mediate the horizontal transfer of information in specific recipient cells by diffusing into neighboring cells or via systemic transport to distant anatomical locations [11]. Furthermore, exosomes can directly modify the invasive capacity of tumor cells by serving as a conduit for signals that initiate EMT [12] and change the cellular physiology of surrounding and distant non-tumor cells to allow the dissemination of cancer cells [13].

MiRNAs can negatively regulate gene expression at the posttranscriptional level by binding to their target mRNAs through base pairing to the 3′-untranslated region (UTR), causing translational repression of the mRNA [14]. Several mechanisms leading to abnormal expression of miRNAs in cancer have been reported, such as chromosome rearrangements and epigenetic modifications [15,16]. Chou et al., showed that dysregulated miRNAs in the stromal compartment could reprogram normal fibroblasts into tumor-promoting CAFs, which could enhance ovarian cancer cells metastasis [17]. In addition, fibroblasts in the tumor microenvironment can "communicate" with tumor cells through the transfer of miRNAs encapsulated in exosomes [18]. To date, no study has been conducted on the miRNAs expression profiles of exosomes derived from CAFs in patients with OSCC. The present study aimed to clarify the role of miRNAs encapsulated in the exosomes derived from CAFs and their potential signaling cascade in OSCC progression.

2. Materials and methods

2.1. Isolation of primary human fibroblasts and OSCC cell culture

Primary human CAFs and donor-matched NFs were isolated from OSCC patients treated by surgical resection at the Department of Oral and Maxillofacial Surgery, Guanghua School of Stomatology, Hospital of Stomatology, Sun Yat-sen University. The isolation and culture of primary human fibroblasts was performed as previously described [19]. Primary fibroblasts isolated from tumor tissues were termed CAFs, and those from the paired normal tissues were termed NFs. Cell purity was assessed by vimentin, FAP, and α-SMA immunofluorescence and western blotting. All primary fibroblasts used in this study were between passages 2 and 5. The use of these clinical samples was approved by the Ethics Committee of Guanghua School of Stomatology, Hospital of Stomatology, Sun Yat-sen University (Approval number: ERC-[2016]-37).

Human oral keratinocytes (HOK) were purchased from ScienCell and cultured in oral keratinocyte medium, according to the manufacturer's instructions. OSCC cells, including CAL27 and SCC15, were kindly donated by the Department of Central Laboratory, Peking University, School and Hospital of Stomatology. CAL27 cells were incubated in Dulbecco's modified Eagle's medium (DMEM; Gibco, Carlsbad, CA, USA) containing 10% FBS (fetal bovine serum; Gibco), and SCC15 cells were maintained in DMEM/F12 (Gibco) medium supplemented with 10% FBS (Gibco). All cells were incubated at 37 °C in a 5% CO_2 atmosphere.

2.2. Exosome preparation

Exosomes were collected from supernatants of primary fibroblasts (cultured in exosome-free medium) and isolated by ultracentrifugation and sucrose cushion centrifugation. Briefly, cell culture supernatant (48 h, serum-free medium) was cleared (2 × 10 min, 500 ×*g*; 1 × 20 min, 2000 ×*g*; 1 × 30 min, 10,000 ×*g*), centrifuged (90 min, 100,000 ×*g*), washed (phosphate-buffered saline (PBS), 90 min, 100,000 ×*g*) and further purified by sucrose-gradient centrifugation [20]. The retained exosomes were stored at −80 °C. GW4869 (Sigma-Aldrich, St. Louis, MO, USA) at a concentration of 10 mM was used to inhibit exosome release. A transmission electron microscopy (TEM), H-7650 electron microscope (HITACHI, Japan), was used to identify the morphology of exosomes. The preparation of exosomes morphology examination was performed as described previously [13].

2.3. Preparation of lentiviral vector and transfection

Lentiviral plasmids encoding miR-34a-5p, or a negative control, and plasmids encoding wild-type (WT) or mutant (Mut) 3′-UTR *AXL* (encoding AXL receptor tyrosine kinase) were purchased from Genechem (Shanghai, China). MiR-34a-5p mimic and miR-34a-5p mimic-control were produced by GenePharma (Shanghai, China). Transfections of miRNAs were performed using Lipofectamine 2000 (Invitrogen, Carlsbad, CA, USA), according to the manufacturer's instructions.

To create *AXL* and *SNAIL* (encoding Snail family transcriptional repressor 1) overexpressing OSCC cell lines, we transfected OSCC cells with 4 μg of pcDNA3.0-AXL, pcDNA3.0-Snail, or pcDNA3.0-neo vector using Lipofectamine 2000 (Invitrogen). After 24 h, the cells were subjected to selection for stable integrants by exposure for 3 weeks to 200–400 μg/ml G418 (Invitrogen) in complete medium containing 10% FBS. *AXL*, *SNAIL*, and *CTNNB1* (encoding β-catenin) knockdown was achieved by transfection using Lipofectamine RNAiMax (Thermo Scientifc, Lafayette, CO, USA) according to the manufacturer's instructions. ON-TARGETplus Non-targeting Pool siRNA (Thermo Scientifc) served as the control. The cells were then assessed for the overexpression or knockdown of AXL, Snail, and β-catenin using western blotting analysis.

2.4. Immunofluorescence

Cells were fixed with 4% paraformaldehyde for 20 min and treated with 0.1% Triton X-100 for 5 min. The cells were then incubated with anti-human antibody against α-SMA (Abcam, Cambridge, MA, USA, Cat# ab5694), vimentin (Abcam, Cat# ab20346), α-tubulin (Abcam, Cat# ab52866), FAP(Abcam, Cat# ab28244), and β-catenin (Cell Signaling Technology, Danvers, MA, USA, Cat# 8480S) overnight at 4 °C, followed by incubation with antibodies conjugated with fluorescent Alexa Fluor 488 or rhodamine (Cell Signaling Technology) at 37 °C for

60 min. The immunofluorescence was visualized under a fluorescence microscope (LSM 5, Carl Zeiss, Germany).

2.5. Quantitative Real-Time PCR

Total RNA was isolated from OSCC cells using the Trizol reagent (Invitrogen) according to the manufacturer's instructions. Then, 2 μg of total RNA was reverse transcribed into cDNA using a reverse transcription polymerase chain reaction (RT-PCR) system (Promega, Madison, WI, USA). The qRT-PCR was performed on a LightCycler 480 (Roche, Indianapolis, IN, USA) with the Fast Start Universal SYBR Green Master Mix (Roche) according to the manufacturer's instructions. The relative mRNA expression was determined using the comparative Ct (ΔΔCt) method. The data are representative of three independent experiments. The sequences of the primers are shown in Supplementary Table 1.

2.6. miRNA sequencing

After total RNA was isolated from exosomes, small RNAs of 18–30 nt were obtained from 200 μg of total RNA using 15% denaturing polyacrylamide gel electrophoresis (PAGE). After PCR amplification, the products were purified and submitted for sequencing via an Illumina Hi-Seq 2000 platform. Library preparation and miRNA sequencing were performed by Ribobio (Guangzhou, China). Differentially expressed miRNAs with a two fold change in expression were analyzed. Predicted miRNA target genes were detected using the TargetScan, miRTarBase, miRDB, and miRWalk databases.

2.7. Western blotting

Protein extracts were resolved by 10–12% SDS-PAGE, transferred to PVDF membranes, and probed with antibodies against human vimentin (Abcam, Cat# ab20346), FAP (Abcam, Cat# ab28244), AXL (Abcam, Cat# ab72069), phospho-GSK-3β S9 (Abcam, Cat# ab75814), GSK-3β (Abcam, Cat# ab131356), Snail (Abcam, Cat# ab53519), E-cadherin (Cell Signaling Technology, Cat# 14472S), β-catenin (Cell Signaling Technology, Cat# 8480S), phospho-AKT-S473 (Cell Signaling Technology, Cat# 4060S), AKT (Cell Signaling Technology, Cat# 9272S), α-tubulin(Cell Signaling Technology, Cat# 12351S), Histone-H3(Cell Signaling Technology, Cat# 4499S), GAPDH (Cell Signaling Technology, Cat# 5174S).

2.8. Gelatin zymography

Gelatin zymography was used to measure the matrix metalloproteinase (MMP)-2 and MMP-9 activity in the cells, and zymograms were processed as described previously [21]. Lytic bands were analyzed using Image Proplus 5.1 software.

2.9. Functional assay

All OSCC cells used in the functional assays were transfected with the indicated plasmids and stable colonies were selected. The functional assays, including proliferation, migration, and invasion assays, and colony formation assays, were performed as described previously [2,19].

2.10. Luciferase reporter assay

A luciferase reporter gene assay was used to verify whether *AXL* was the direct target gene of miR-34a-5p. Luciferase reporter constructs encoding the wild-type 3′ untranslated regions of AXL (AXL-3′UTR-WT) or mutant 3′ UTRs of AXL (AXL-3′UTR-MUT) were synthesized by Genechem (Shanghai, China). The 3′-UTR luciferase vector (150 ng) was cotransfected into OSCC cells co-transfected with either miR-34a-5p mimic or miR-34a-5p mimic-control using Lipofectamine 2000 (Invitrogen). After incubation for 48 h, the cells were collected and lysed, and their luciferase activities were detected by the Dual-Luciferase Reporter Assay Kit (Beyotime Biotechnology, Shanghai, China) according to the manufacturer's protocol.

2.11. In situ hybridization

In situ hybridization (ISH) was performed on 4 μm paraffin sections to detect miR-34a-5p in OSCC and paired normal tissue by a in situ hybridization kits (Exon Biological Technology, Guangzhou, China). ISH was performed as previously described [22].

2.12. Animal models

BALB/c nude mice (Beijing Vital River, Beijing, China) at 4–6 weeks of age were used. OSCC cells (5×10^6 cells/body) and fibroblasts (5×10^6 cells/body) were injected subcutaneously. Mice were sacrificed 6 weeks after tumor inoculation or if they showed signs of distress. After sacrifice, the tumors were dissected, collected, and weighed. The research was approved by the Ethical Committee on Animal Research of the Sun Yat-sen University. All experimental procedures were performed according to national guidelines regarding the care and use of laboratory animals.

The tumor tissues were used for immunohistochemistry study for E-cadherin (Cell Signaling Technology, Cat# 14472S), vimentin (Abcam, Cat# ab20346), Snail (Abcam, Cat# ab53519), β-catenin (Cell Signaling Technology, Cat# 8480S), MMP-2 (Abcam, Cat# ab37150), MMP-9 (Abcam, Cat# ab73734), and AXL (Abcam, Cat# ab72069). Serial sections (4-μm thick) were cut, and hematoxylin and eosin (H&E) and immunostaining were performed, as described previously [2]. Image Proplus 5.1 software was used to analyze the area and intensity of positive staining in five random regions and then the average value per field was used to evaluate the protein expression level.

2.13. Statistical analysis

The experimental data were analyzed using SPSS version 13.0 software (SPSS, Chicago, IL, USA). The results are expressed as the mean ± standard deviation (SD). The statistical significance of the differences was analyzed using a two-tailed Student's *t*-test or one-way analysis of variance. $P < .05$ was considered significant.

3. Results

3.1. Characteristics of fibroblast-derived exosomes from patients with OSCC

We isolated primary NFs and CAFs from patients with OSCC who underwent tumor resection, using the tissue block method. Both NFs and CAFs showed a spindle-like morphology and could be grown for at least 12 passages (Fig. 1A). We performed western blotting to characterize the phenotypes of NFs and CAFs, and analyzed the expression of vimentin, FAP, and α-SMA. We found that both NFs and CAFs were positive for vimentin and that the expression of FAP and α-SMA in CAFs was higher than that in NFs (Fig. 1B). These biomarker expression changes were verified using immunofluorescence. Under a confocal microscope, we found that the FAP and α-SMA immunofluorescence staining were much higher in CAFs than in NFs (Fig. 1C).

To determine whether exosomes could be released from NFs and CAFs, we incubated both cells in exosome-free medium. The exosomes in the conditioned media were isolated using serial centrifugation and filtration. The exosome pellets were resuspended in PBS and then examined by transmission electron microscopy (TEM). Their size was within the characteristic diameter range of 40–120 nm (Fig. 1D). We then characterized the exosomes using western blotting for the well-recognized markers CD63 and GM130 (Golgi matrix protein GM130). As shown in Fig. 1E, the exosomes lacked GM130, which was detected in the cell

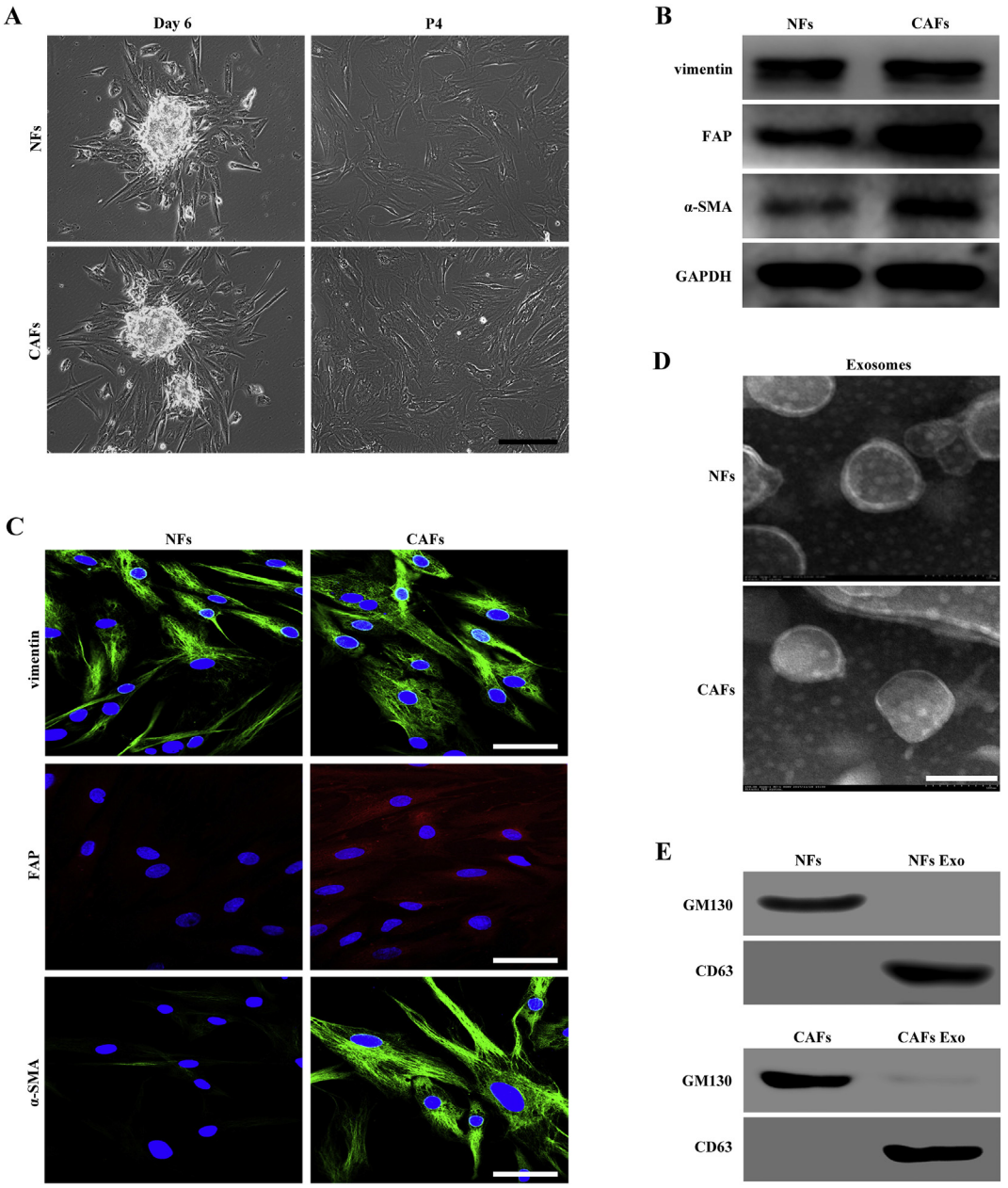

Fig. 1. Characteristics of fibroblasts derived from patients with OSCC and isolation of exosomes. (A) Representative morphology of NFs and CAFs derived from patients with OSCC. Scale bar, 200 μm. (B) Western blotting analysis of the expression of CAF markers (α-SMA and FAP) and fibroblasts marker (vimentin) in isolated fibroblasts. (C) Immunofluorescence staining identification of CAFs using antibodies against vimentin, α-SMA, and FAP. Scale bar, 100 μm. (D) Transmission electron microscopy (TEM) showing exosomes isolated from NFs and CAFs-conditioned medium. Scale bar, 100 nm. (E) Western blotting analysis of the exosome marker CD63 and the Golgi matrix protein GM130 in exosome-enriched conditioned medium.

lysate; CD63 was not detected in whole cell lysate but was found in abundance in the exosomal fraction. Based on their size and the presence of CD63, we confirmed that the vesicles isolated from the conditional media were exosomes.

3.2. CAFs transfer miR-34a-5p-devoid exosomes to OSCC cells

Previous studies have reported that cancer cells secrete exosomes in great amounts and transfer cancer-associated signaling molecules to surrounding cells [23]. Post-transcriptional gene expression in recipient cells can be regulated by microRNAs contained in exosomes [24]. In the present study, we analyzed the microRNA profiles of exosomes derived from NFs and CAFs via Ion Torrent/MiSeq sequencing. As shown in Fig. 2A and B, the miRNA level in exosomes from CAFs was decreased significantly compared with that in NFs. Among the 31 significantly downregulated and 12 significantly upregulated miRNAs in the CAF-derived exosomes, miR-34a-5p has been reported to be downregulated in primary colorectal cancer (CRC) tissue and inhibits the recurrence of CRC in a p53-dependent manner [25]. In osteosarcoma (OS), miR-34a-5p promoted OS multi-chemoresistance via downregulating the Deltalike ligand 1 (DLL1) gene, the ligand of the Notch pathway, and thus negatively correlates with OS chemoresistance [26]. In the present study, real-time PCR was conducted to detect miR-34a-5p expression in six CAFs and matched NFs. Interestingly, we found that the expression of miR-34a-5p was lower in CAFs than in NFs (Fig. 2C). H&E staining and ISH of sequential sections further confrmed that the level of miR-34a-5p was much lower in tumor fibroblasts than in normal fibroblasts (Fig. 2D). Therefore, we selected miR-34a-5p (downregulated) for furhter study.

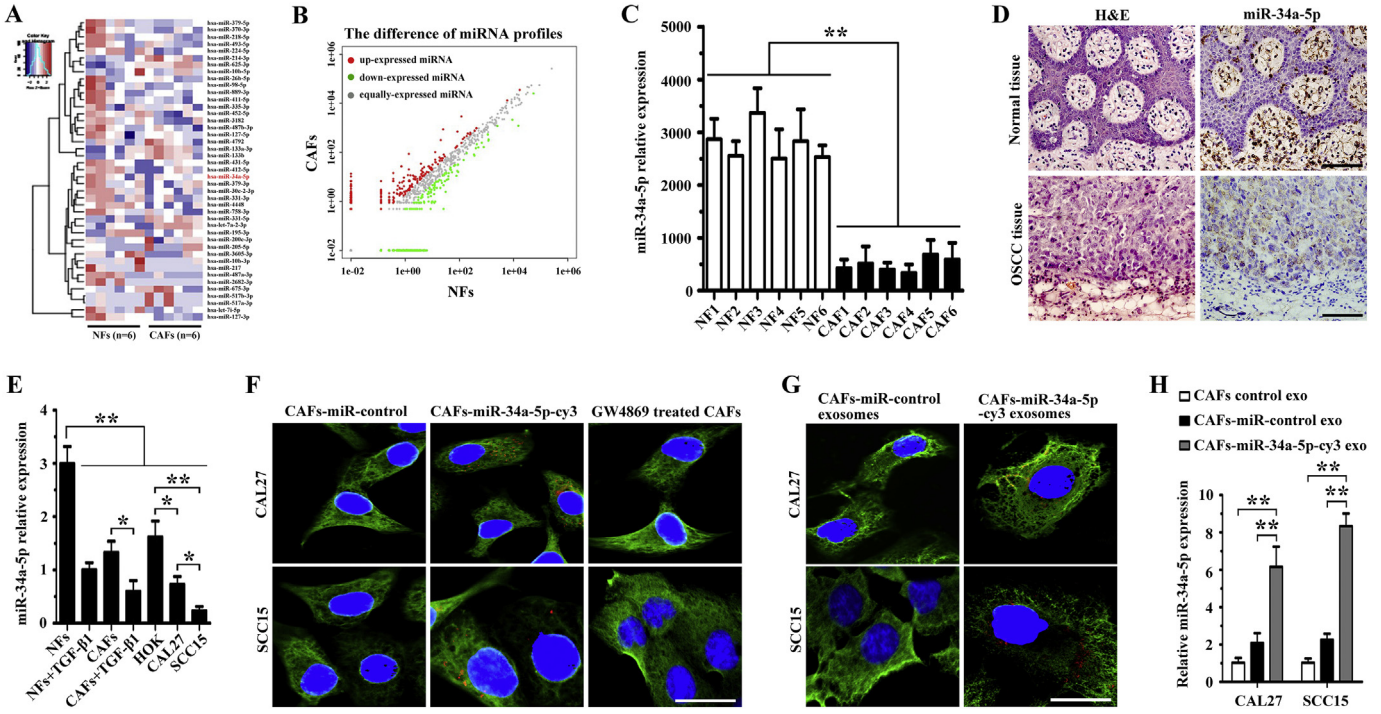

Fig. 2. OSCC cells absorb miR-34a-5p-devoid exosomes derived from CAFs. (A) Heatmap diagram of differential miRNA expression profiles between CAFs and NFs-derived exosomes. Red = miRNAs with higher expression, blue = miRNAs with lower expression, and white = miRNAs with equal expression. (B) Differential miRNA expression profiles between CAFs and NFs-derived exosomes. Red = miRNAs with higher expression, green = miRNAs with lower expression, and gray = miRNAs with equal expression. (C) Real-time PCR analysis of miR-34a-5p expression in NFs and CAFs ($n = 6$). $^{**}P < .01$. (D) Representative H&E and ISH staining of miR-34a-5p in OSCC and donor-matched normal tissue. Scale bar, 200 μm. (E) Real-time PCR analysis of miR-34a-5p expression in HOK, CAL27, SCC15, NFs, and CAFs, and 5 ng/ml TGF-β1-stimulated NFs and CAFs. $^{*}P < .05$; $^{**}P < .01$. (F) CAFs transfected with cy3-tagged miR-34a-5p (CAFs-miR-34a-5p-cy3) or with the miR-control, and GW4869-treated CAFs were indirectly co-cultured with OSCC cells for 24 h. Fluorescence microscopy was used to detect the α-tubulin (green) and cy3 (red) fluorescent signals in OSCC cells. Scale bar, 100 μm. (G) Exosomes were isolated from conditioned media derived from CAFs transfected with cy3-labeled miR-34a-5p (CAFs-miR-34a-5p-cy3 exo) or with miR-control (CAFs-miR-control exo) and 200 μg of exosomes were added to OSCC cells for 24 h. Fluorescence microscopy was used to detect the α-tubulin (green) and cy3 (red) fluorescent signals in OSCC cells. Scale bar, 100 μm. (H) Real-time PCR analysis of miR-34a-5p expression in OSCC cells treated with 200 μg of exosomes derived from CAFs (CAFs control exo) and from CAFs transfected with a lentiviral plasmid containing pre-miR-34a-5p (CAFs-miR-34a-5p exo) or with the miR-control (CAFs-miR-control exo). $^{**}P < .01$.

Transforming growth factor beta (TGF-β) can activate NFs to differentiate into CAFs. Therefore, we used 5 ng/ml TGF-β1 to stimulated NFs and CAFs for 48 h and measured the expression of miR-34a-5p in TGF-β1-treated fibroblasts. As shown in Fig. 2E, we found that TGF-β1-treated fibroblasts (NFs and CAFs) expressed a lower level of miR-34a-5p than the control group (untreated fibroblasts). We then measured the expression of miR-34a-5p in human OSCC cell lines, CAL27 and SCC15, and in human oral keratinocytes (HOK). The results indicated that both OSCC cell lines expressed lower levels of miR-34a-5p than HOK, and that SCC15 cells expressed lower levels of miR-34a-5p than CAL27 cells (Fig. 2E).

To examine whether CAF-derived exosomes could be transferred to OSCC cells, we cultured OSCC cells in cell culture medium supplemented with exosome-depleted serum for 3 days, and then co-cultured OSCC cells with CAFs transfected with cy3-tagged miR-34a-5p indirectly. We then used fluorescence microscopy to observe red fluorescence of cy3 and green fluorescence of α-tubulin in CAL27 and SCC15 cells. We found that OSCC cells took up cy3-tagged miR-34a-5p, and the red fluorescence of cy3 was abolished when CAFs were treated with GW4869, an exosome inhibitor (Fig. 2F). Exosomes were then isolated from the CAFs transfected with cy3-tagged miR-34a-5p. After addition of the isolated cy3-tagged exosomes to OSCC cells and incubation for 24 h, we examined them under a fluorescence microscopy. We found that red fluorescent signals could be detected in the recipient OSCC cells (Fig. 2G).

We transfected a lentiviral plasmid containing pre-miR-34a-5p into CAFs and isolated exosomes from CAFs, CAFs-miR-control, and CAFs-miR-34a-5p. Next, we incubated those exosomes with OSCC cells. Using real-time PCR, we found that the expression of miR-34a-5p in OSCC incubated with exosomes from CAFs-miR-34a-5p was much higher than that in OSCCs incubated with exosomes from both CAFs and CAFs-miR-control groups (Fig. 2H). Taken together, these results showed that OSCC cells could absorb miR-34a-5p-devoid exosomes from CAFs.

3.3. MiR-34a-5p influences tumor cell proliferation and metastasis in vitro and in vivo

To determine the effect of miR-34a-5p on cellular behavior, we transfected CAL27 and SCC15 cells with a lentiviral plasmid containing pre-miR-34a-5p. The CCK-8 assays revealed that miR-34a-5p significantly reduced the rate of cell proliferation in CAL27 and SCC15 cells compared with that in the miR-control transfected group (Fig. 3A). Using a colony formation assay, we also found that miR-34a-5p overexpression could significantly reduce the colony counts of both CAL27 and SCC15 cells (Fig. 3B).

Next, we explored whether miR-34a-5p influenced the migration and invasion of OSCC cells. We used a Transwell assay to determine the impact of miR-34a-5p on OSCC cell mobility. We found that miR-34a-5p overexpression could suppress the migration of both CAL27 and SCC15 cells (Fig. 3C). We also found that the number of invaded CAL27-miR-34a-5p cells and SCC15-miR-34a-5p cells was much lower than that in the miR-control group (Fig. 3D).

Using an immunodeficient BALB/c mice subcutaneous tumor model to determine the tumorigenesis of miR-34a-5p transfected OSCC cells, we found that the mean weight of tumor nodules in the SCC15 miR-34a-5p overexpression group was lower than in the miR-control group (Fig. 3E). Next, CAL27 cells were co-injected with NFs, CAFs-

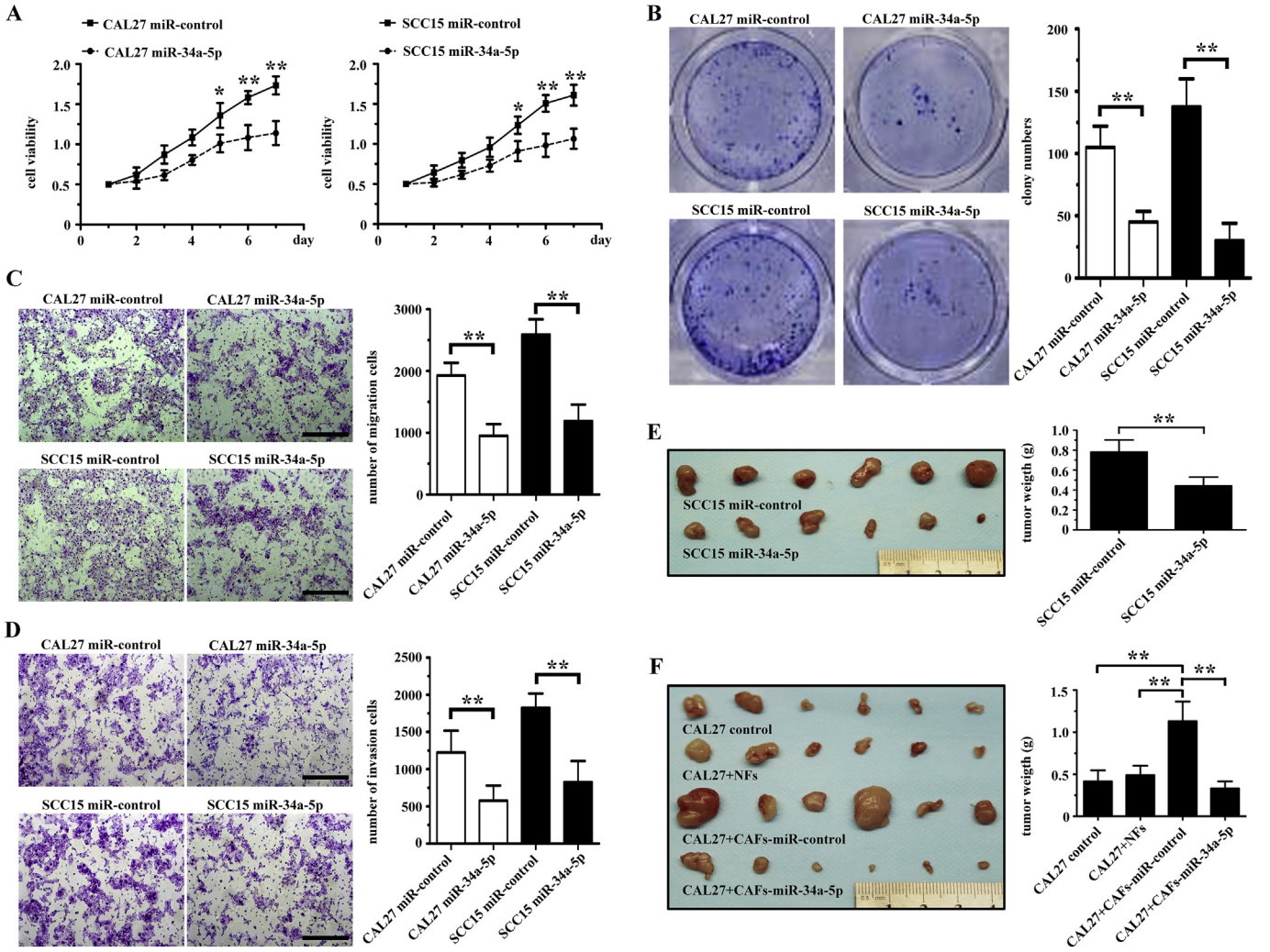

Fig. 3. MiR-34a-5p inhibits OSCC cell proliferation, colony formation, migration, and invasion both in vitro and in vivo. (A) The effect of miR-34a-5p overexpression on the growth rate of both CAL27 and SCC15 cells examined using the CCK-8 assay. $^{*}P < .05$; $^{**}P < .01$. (B) The effect of miR-34a-5p overexpression expression on colony formation in both CAL27 and OSCC15 cells examined using the colony formation assay. $^{**}P < .01$. (C-D) The effect of miR-34a-5p overexpression on the migration (C) and invasion (D) of both CAL27 and OSCC15 cells examined using a Transwell assay. Scale bar, 200 μm. $^{**}P < .01$. (E) SCC15 cells transfected with the lentiviral plasmid containing pre-miR-34a-5p or miR-control were injected subcutaneously into nude mice (n = 6). After 6 weeks, the mice were euthanized, and the tumors were excised. $^{**}P < .01$. (F) CAL27 cells were coinjected with NFs, CAFs-miR-control, or CAF-miR-34a-5p into nude mice subcutaneously. After 6 weeks, the mice were euthanized, and the tumors were excised. $^{**}P < .01$.

miR-control, or CAF-miR-34a-5p into immunodeficient BALB/c mice subcutaneously. We found that NFs did not promote the tumorigenicity of CAL27 cells, and that the tumorigenicity of CAL27 cells in CAFs-miR-34a-5p group was lower than that in the CAFs-miR-control group (Fig. 3F). Furthermore, NFs or CAFs alone did not form tumors in the nude mice (Supplementary Figs. 1A and 1B). These results indicated that CAFs-miR-34a-5p suppressed the tumorigenicity of cancer cells through the transfer of exosomal miR-34a-5p to OSCC cells.

3.4. AXL is a direct target of miR-34a-5p

Four publicly available bioinformatics tools (TargetScan, miRTarBase, miRDB and miRWalk) were used to analyze genes targeted by miR-34a-5p (Fig. 4A). Among the predicted genes, *AXL*, which has been reported to be a logical molecular target in head and neck squamous cell carcinoma [27] and is associated with cell-cell adhesion and stemness of cancer cells [28], was chosen for further study. Western blotting showed that the expression of AXL was significantly lower in CAL27 and SCC15 cells transfected with a lentiviral plasmid expressing miR-34a-5p than in the miR-control group (Fig. 4B). After incubation with CAFs-exo (CAFs-derived exosomes), CAFs-miR-control-exo (exosomes from CAFs transfected with miR-control), or CAFs-miR-34a-5p-exo (exosomes from CAFs overexpressing miR-34a-5p), we found that the mRNA level of *AXL* in the CAFs-miR-34a-5p-exo treated CAL27 and SCC15 cells groups was significantly lower than that in the CAFs-exo group and CAFs-miR-control-exo group (Fig. 4C). Fig. 4D shows the predicted miRNA binding sites in the 3′ UTR of *AXL*. We used a luciferase reporter assay to determine whether miR-34a-5p could target the 3′ UTR of *AXL* directly. We cloned the 3′ UTR fragment (WT-AXL) of *AXL* containing a miR-34a-5p binding site and mutant fragments (MUT-AXL) into luciferase reporter vectors. We found that miR-34a-5p could significantly reduce WT-AXL luciferase activity in both CAL27 and SCC15 cells, and that miR-34a-5p had no effect on the luciferase activity of MUT-AXL group (Fig. 4E).

3.5. AXL mediates the proliferation and motility of OSCC cells

Western blotting and real-time PCR analysis showed that AXL expression was higher in SCC15 cells than in CAL27 cells (Supplementary Figs. 2A and 2B). In Transwell assays, SCC15 cells showed higher motility than CAL27 cells (Supplementary Fig. 2C). To further investigate whether miR-34a-5p exerted its effects in targeting *AXL* in OSCC cells, we knocked down the expression of *AXL* using short interfering RNAs

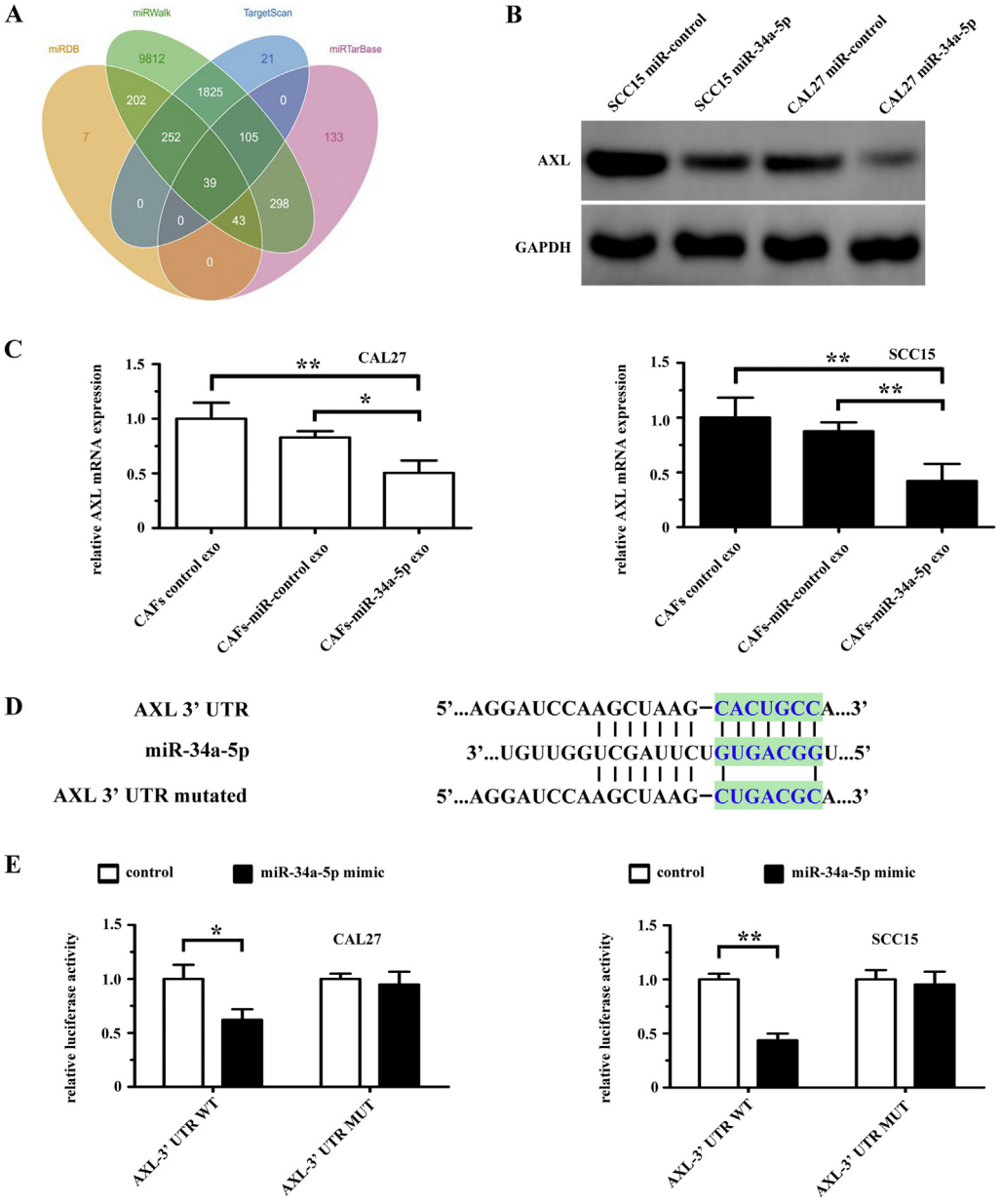

Fig. 4. *AXL* is a direct target of miR-34a-5p in OSCC cells. (A) The target genes of miR-34a-5p were predicted using publicly available bioinformatics tools (TargetScan, miRWalk, miRTarBase, and miRanda). (B) The expression of AXL in both CAL27 and SCC15 cells was examined using western blotting after transfection with lenti-miR-control or lenti-miR-34a-5p. (C) *AXL* mRNA levels in CAL27 and SCC15 cells treated with exosomes derived from CAFs control, CAFs-miR-control or CAFs-miR-34a-5p were examined using real-time PCR. $^{*}P < .05$; $^{**}P < .01$. (D) Predicted miR-34a-5p binding sites in the 3′ UTR of wild-type (AXL-3′-UTR-WT) and mutant (AXL-3′-UTR-MUT) AXL sequences. (E) Luciferase reporter assays were performed 48 h after co-transfection of CAL27 and SCC15 cells with control or miR-34a-5p mimics and a luciferase vector encoding the wild-type or mutant *AXL* 3′ UTR region. $^{*}P < .05$; $^{**}P < .01$.

(siRNAs) in SCC15 cells and overexpressed *AXL* using a plasmid containing the full-length *AXL* cDNA (AXL-OE) in CAL27 cells. Western blotting showed that the level of AXL was downregulated in both the si-AXL #1 and si-AXL #2 groups, and the level of AXL was upregulated in the AXL-OE group (Fig. 5A). The colony formation, proliferation, and mobility of SCC15 cells decreased significantly after *AXL* knockdown, and *AXL* overexpression increased the colony formation, proliferation, and mobility of CAL27 cells (Figs. 5B-5E).

Next, we transfected both a lentiviral plasmid containing pre-miR-34a-5p and a plasmid containing full-length *AXL*. AXL overexpression counteracted the effects of miR-34a-5p in CAL27 cells (Figs. 5F-5H). Similar results were obtained in the SCC15 cells experiment (Supplementary Figs. 3A-3C).

3.6. The AKT/GSK-3β/β-catenin/Snail signaling cascade mediates the effects of the miR-34a-5p/AXL axis on OSCC cells

MiR-34a-5p affects the proliferation and motility of OSCC cells; therefore, we further investigated the underlying mechanism. Overexpression of miR-34a-5p in CAL27 cells could decrease the amount of active β-catenin in the nucleus (Fig. 6A). Moreover, these effects of overexpressing miR-34a-5p could be rescued by upregulating *AXL* expression ectopically (Fig. 6A). Meanwhile, immunofluorescence staining showed that miR-34a-5p overexpression markedly decreased the activation of β-catenin in the nucleus, and that AXL overexpression could upregulate the activation of β-catenin (Fig. 6B). Next, we examined the phosphorylation status of GSK-3β and AKT in miR-34a-5p

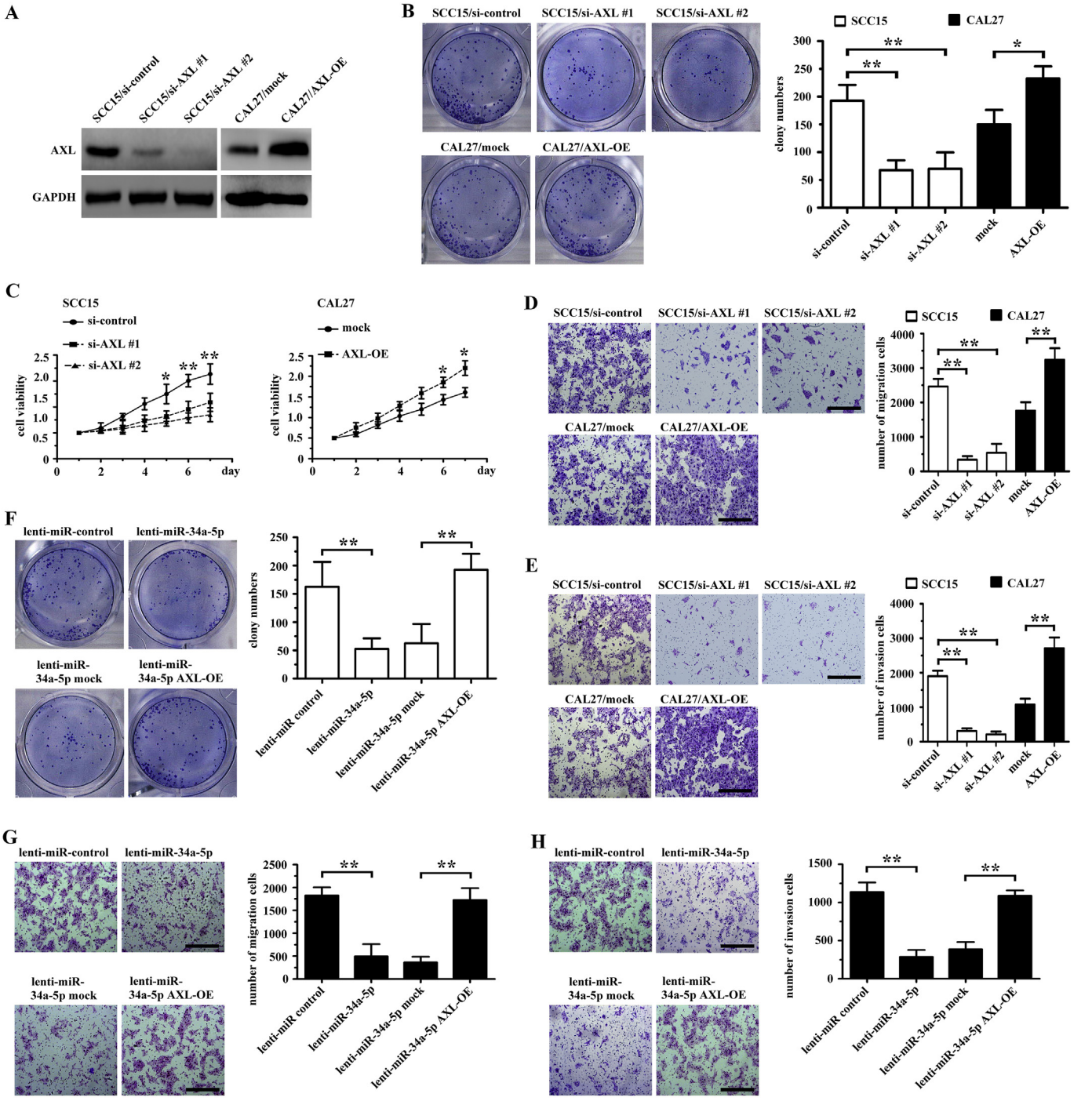

Fig. 5. MiR-34a-5p inhibits OSCC cell proliferation, migration, and invasion by targeting *AXL*. (A) AXL expression in OSCC cells transfected with *AXL* was examined by western blotting. (B) Colony formation in both *AXL*-transfected CAL27 and SCC15 cells was examined using a colony formation assay. $^{*}P < .05$; $^{**}P < .01$. (C) The growth rate of *AXL*-transfected CAL27 and SCC15 cells was examined using the CCK-8 assay. $^{*}P < .05$; $^{**}P < .01$. (D-E) The migration (D) and invasion (E) of *AXL*-transfected CAL27 and SCC15 cells was examined using a Transwell assay. $^{**}P < .01$. (F-H) Clone formation (F), migration (G), and invasion (H) of CAL27 cells transfected with lenti-miR-control, lenti-miR-34a-5p, lenti-miR-34a-5p mock and lenti-miR-34a-5p AXL-OE was examined using a colony formation assay and Transwell assay, respectively. $^{**}P < .01$.

and AXL-transfected CAL27 cells. We found that overexpression of miR-34a-5p markedly suppressed the phosphorylation of GSK-3β and AKT in CAL27 cells, consequently causing a decrease in vimentin levels and an increase in the expression of E-cadherin (Fig. 6C). However, AXL overexpression in miR-34a-5p transfected CAL27 cells antogonized the effect of miR-34a-5p on the phosphorylation of GSK-3β and AKT (Fig. 6C).

To further investigate the impact of AXL on the AKT/GSK-3β/β-catenin signaling pathway, we used two target-specific siRNAs to downregulate the expression of *AXL* in CAL27 cells. A marked decrease in active GSK-3β, active β-catenin, active AKT, and vimentin, and upregulation of E-cadherin was observed after AXL knockdown. Furthermore, the overexpression of AXL in CAL27 cells caused an opposite effect (Fig. 6D).

Snail is a transcription factor that plays an important role in epithelial-mesenchymal transition (EMT) and a previous study found that β-catenin/TCF4 could activate *SNAIL* transcription [29]. We further determined whether Snail was the functional mediator of AXL. Knockdown of endogenous AXL or β-catenin in CAL27 cells drastically

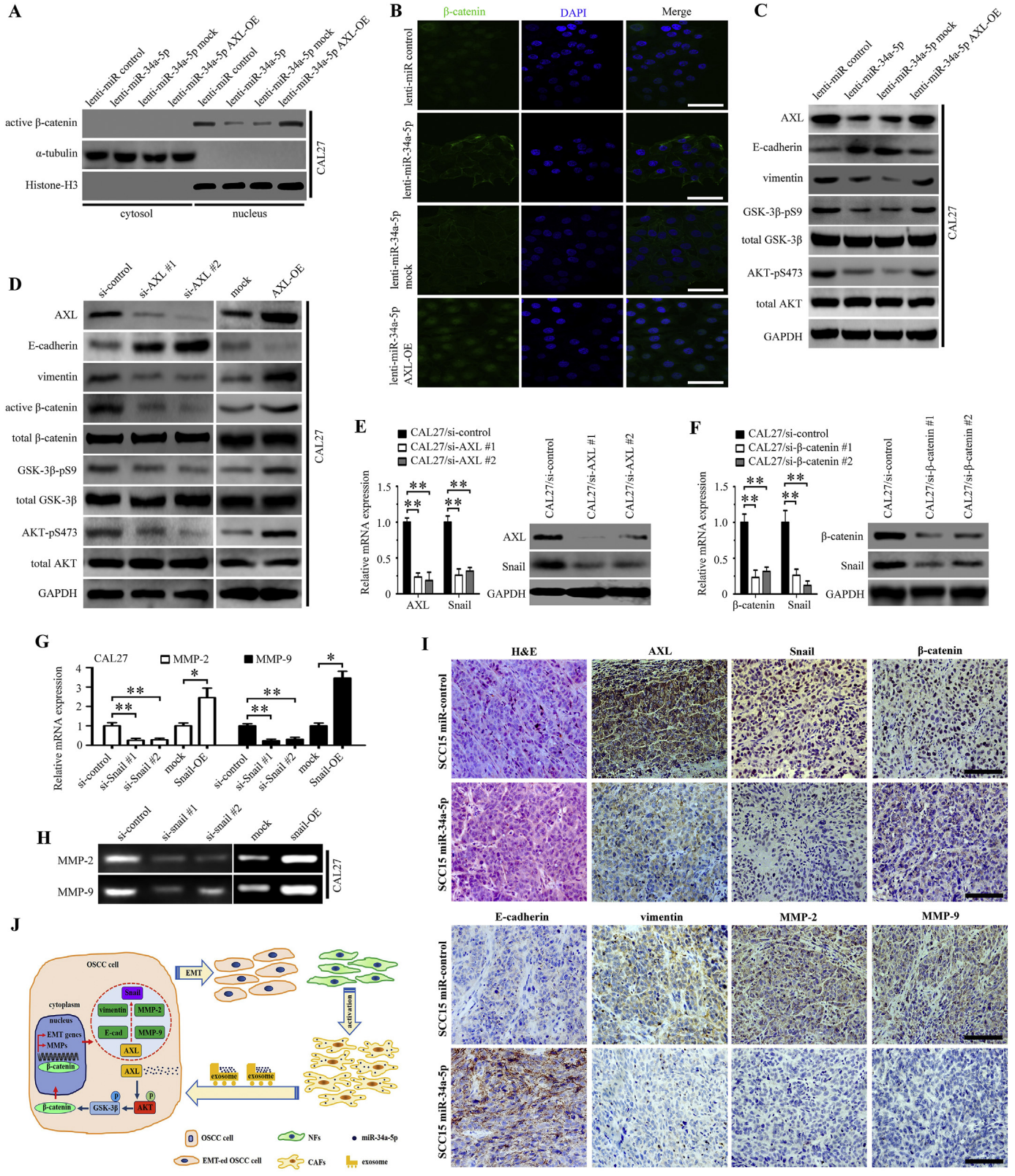

Fig. 6. MiR-34a-5p exerts its functions by inhibiting EMT and MMP-2/9 activation in OSCC cells. (A-B) The activation of β-catenin in CAL27 cells transfected with lenti-miR-control, lenti-miR-34a-5p, lenti-miR-34a-5p mock, and lenti-miR-34a-5p AXL-OE was examined using western blotting (A) and immunofluorescence staining (B); scale bar, 100 μm. (C) The effect of lenti-miR-control, lenti-miR-34a-5p, lenti-miR-34a-5p mock, and lenti-miR-34a-5p AXL-OE transfection in CAL27 cells on AKT/GSK-3β/β-catenin signaling pathway was examined using western blotting. (D) The effect of two target-specific *AXL* siRNAs transfection and *AXL* overexpression in CAL27 cells on the AKT/GSK-3β/β-catenin signaling pathway was examined using western blotting. (E-F) The expression of Snail was detected in CAL27 cells transfected with si-AXL (E) or si-β-catenin (F) was examined using real-time PCR and western blotting, respectively. $^{**}P < .01$. (G-H) The activation of MMP-2 and MMP-9 in CAL27 cells transfected with the *Snail* siRNA and the vector containing full-length *Snail* in CAL27 was examined by real-time PCR (G) and Gelatin zymography (H). $^{*}P < .05$; $^{**}P < .01$. (I) Representative H&E and immunohistochemical staining for AXL, Snail, β-catenin, E-cadherin, vimentin, MMP-2 and MMP-9 in miR-34a-5p overexpression in SCC15 cells xenograft tumor tissue; scale bar, 200 μm. (J) Schematic representation of the contribution of miR-34a-5p-devoid exosomes derived from CAFs to EMT in OSCC cells via AKT/GSK-3β/β-catenin/Snail signaling cascade.

downregulated Snail expression at both the mRNA and protein levels (Fig. 6E and F). In Snail-transfected CAL27 cells, but not in the control group, we observed obvious MMP-2 and MMP-9 downregulation in Snail-silenced cells and that Snail overexpression upregulated the expression levels of MMP-2 and MMP-9 (Fig. 6G and H). Similar results were observed in the SCC15 cells experiment (Supplementary Figs. 4A-4H). Furthermore, we found that Snail RNAi treatment enhanced the expression of E-cadherin and decreased the expression of vimentin in both CAL27 and SCC15 cells, and that Snail overexpression upregulated the expression of vimentin and decreased the expression of E-cadherin (Supplementary Figs. 5A-5D). Moreover, we used immunohistochemical staining to evaluate the expression levels of AXL, Snail, β-catenin, E-cadherin, vimentin, MMP-2, and MMP-9 in the tumors produced by SCC15 miR-control cells and SCC15 miR-34a-5p cells in nude mice. We found that the expression levels of AXL, β-catenin, Snail, vimentin, MMP-2, and MMP-9 were decreased in the miR-34a-5p overexpressing group, and the expression of E-cadherin was elevated at the same time. Representative H&E and immunohistochemical staining of subcutaneous tumor are shown in Fig. 6I.

Taken together, our data indicated that the miR-34a-5p/AXL axis promotes EMT and cell invasion through the AKT/GSK-3β/β-catenin signaling pathway, leading to transcriptional upregulation of *SNAIL* and the activation of both MMP-2 and MMP-9 (Fig. 6J). Our results demonstrated that the miR-34a-5p/AXL axis might represent a therapeutic target in OSCC.

4. Discussion

Mounting evidence suggests that miRNAs transferred by exosomes modulate the tumor microenvironment [13,30]. In present study, we used miRNA-seq to compare the miRNA profiles of exosomes derived from six paired NFs and CAFs from patients with oral squamous cell carcinoma (OSCC). Our research demonstrated that miR-34a-5p was significantly downregulated in the CAFs-derived exosomes, and that exosomes derived from CAFs could be transferred to OSCC cells. Furthermore, we found that miR-34a-5p could suppress OSCC cell proliferation and motility by targeting *AXL*. These findings suggested that miR-34a-5p-devoid exosomes derived from CAFs contribute to the malignant progression of OSCC.

In recent years, many studies have shown that CAFs enhance the invasion in breast cancer, non-small-cell lung cancer, and basal cell carcinoma [31–34]. CAFs promote tumor progression through specific communications with cancer cells. Jing et al. reported that epithelial ovarian cancer (EOC) cells activate NFs via transforming growth factor-β1 (TGF-β1) signaling, and that CAFs contribute to the invasion and adhesion of EOC cells [35]. Fullár et al. reported that the fibroblast-produced inactive MMP-2 is activated by the tumor-cell-produced membrane-type 1 matrix metalloproteinase (MT1-MMP), and that the activated MMP-2 is essential for the fine-tuning of cancer cells invasion [36]. However, the mechanism underlying the influence of CAFs on OSCC progression has not been fully demonstrated.

Although many studies have demonstrated that CAFs communicate with tumor cells via secreting growth factors and producing ECM-degrading proteases [37], other studies have shown that exosomes are important mediators of cancer progression [38–40]. Singh et al. showed that miR-10b-carrying exosomes could be transferred among different breast cancer cell lines through direct absorption, and that treatment with exosomes derived from MDA-MB-231 cells could induce the invasion ability of non-malignant human mammary epithelial cells [41]. In this study, we compared the miRNA profiles of exosomes from six paired NFs and CAFs from patients with OSCC. Among the 43 miRNAs that were present at significantly different levels between NFs and CAFs exosomes, we identified miR-34a-5p for further study. To the best of our knowledge, this study is the first to analyze the exosomal miRNA profile of fibroblasts in OSCC. Our results showed that the expression of miR-34a-5p in NFs was downregulated when they were treated with TGF-β1. We also found that overexpression of cy3-labeled miR-34a-5p in CAFs leads to an increase of exosomal miR-34a-5p in the OSCC cells, suggesting that oral cancer cells absorb CAFs-derived miR-34a-5p via exosomes. Increasing evidence indicates that secreted miRNAs have a significant impact in a variety of physiological and pathological conditions. Fabbri et al. showed that miR-21 and miR-29a, secreted from cancer cells, trigger inflammatory responses that may promote tumor growth and metastasis [42]. Zhang et al. showed that CAFs enhance the malignant phenotype transition of hepatocellular carcinoma through transferring miR-320a-devoid exosomes to cancer cells, and that the miR-320-PBX3 axis increases the motility of hepatocellular carcinoma cells via activating the MAPK pathway [43]. Although studies have shown the effect of dysregulated miR-34a-5p in colorectal cancer [25] and osteosarcoma [26,44], the underlying mechanisms of miR-34a-5p in OSCC progression have not been elucidated. Our study provides evidence that miR-34a-5p overexpression could inhibit the proliferation and motility of OSCC cells in vitro and in vivo. To confirm the effects of CAFs-derived miR-34a-5p-devoid exosomes on tumorigenicity of OSCC cells, we co-injected CAL27 cells with CAFs overexpressing miR-34a-5p into nude mice. We found that CAFs-miR-34a-5p significantly inhibited tumor growth in vivo. These results strongly suggested that CAFs mediate the proliferation and motility of OSCC cells by transferring miR-34a-5p-devoid exosomes to cancer cells. In our search for a direct target for miR-34a-5p, we performed bioinformatics analysis and identified a sequence complementary to miR-34a-5p in the 3′ UTR region of the *AXL* mRNA. Furthermore, we found that ectopic expression of miR-34a-5p significantly downregulated the expression of *AXL* in OSCC cells.

AXL, belonging to the TAM family (Tyro3, Mer, AXL) of receptor tyrosine kinases, regulates several aspects of cell survival, proliferation, motility, and adhesion [45,46]. Increased expression of AXL has been reported in several human cancers, such as colon, esophageal, thyroid, breast, lung, liver, and astrocytoma–glioblastoma [47]. In the present study, we found that reintroduction of AXL in miR-34a-5p-overexpressing OSCC cells antagonized the effect of miR-34a-5p on the proliferation and motility of OSCC cells, suggesting that the miR-34a-5p/AXL axis plays an important role in OSCC progression.

Next, we investigated the possible downstream pathway of the miR-34a-5p/AXL axis. We found that overexpression of miR-34a-5p markedly downregulated the expression of vimentin and increased that of E-cadherin, suggesting that the miR-34a-5p/AXL axis mediated the progression of OSCC via epithelial-mesenchymal transition (EMT). EMT is important in embryogenesis, as well as in carcinogenesis, and is mainly responsible for single cell invasion, during which cancer cells not only change their shapes and adhesive properties, but also lose the expression of epithelial markers and acquire mesenchymal signatures [27,48]. As an important driver of EMT, the accumulation and nuclear import of β-catenin could interact with T-cell factor/lymphoid enhancer factor (TCF/LEF) and induce the expression of genes responsible for the EMT process [29]. We further validated that EMT in miR-34a-5p and AXL-transfected OSCC cells was associated with the activation of the AKT/GSK-3β/β-catenin signaling pathway. Interestingly, AXL and β-catenin knockdown decreased the expression of Snail, a canonical EMT-inducing transcription factor. Several independent studies showed that EMT-inducing transcription factors could induce the expression of AXL, which further upregulated the expression of Twist, Snail, and Slug via a positive feedback loop [49,50]. In present study, we validated that the AKT/GSK-3β/β-catenin signaling pathway was responsible for miR-34a-5p/AXL-mediated OSCC progression. More importantly, we found that Snail was transcriptionally upregulated by β-catenin, whose accumulation in the nucleus was mediated by the miR-34a-5p/AXL axis. Accumulating evidence indicates that high expression of Snail in patients with OSCC or hepatocellular carcinoma (HCC) is a predictor for shorter survival and poor prognosis [51,52]. Moreover, Snail repressed the expression of RKIP, a tumor metastasis suppressor protein, to promote the metastasis of prostate cancer cells [53]. Our findings

revealed that Snail overexpression promoted EMT in OSCC cells, and that downreguration of Snail caused an opposite effect. Consistent with previous studies, we found that Snail induced OSCC cell invasion via the activation of MMP-2 and MMP-9 [52,54]. Based on the important role of AKT/GSK-3β/β-catenin signaling and EMT, it is reasonable to conclude that there is a complex regulatory network involving the miR-34a-5p/AXL axis, AKT/GSK-3β/β-catenin signaling, and EMT in OSCC. In addition, as an important EMT activator, Snail in the crosstalk between EMT and the miR-34a-5p/AXL axis merits special attention in future studies.

In conclusion, our findings showed that OSCC cells gain a more aggressive phenotype in the tumor microenvironment by taking up miR-34a-5p-devoid exosomes derived from CAFs. In addition, the transfer of miR-34a-5p could affect the proliferation and motility of OSCC cells through the AKT/GSK-3β/β-catenin/Snail signaling cascade (Fig. 6J). These data strongly suggested that miR-34a-5p/AXL axis inhibitors could be potential therapeutics to treat oral squamous cell carcinoma.

Funding sources

This work was supported by the National Natural Science Foundation of China [No. 81602382].

Declaration of interests

The authors have no conflicts of interest to declare.

Author contributions

YYL designed the research and wrote the paper. YWT, GS, and LP performed all the experiments. JMZ assisted with data acquisition and statistical analysis. SEZ and JFL collected the clinical samples. ZYJ supported the animal experiments.

Supplementary data to this article can be found online at https://doi.org/10.1016/j.ebiom.2018.09.006.

References

[1] Warnakulasuriya S. Global epidemiology of oral and oropharyngeal cancer. Oral Oncol 2009;45:309–16.
[2] Li YY, Zhou CX, Gao Y. Moesin regulates the motility of oral cancer cells via MT1-MMP and E-cadherin/p120-catenin adhesion complex. Oral Oncol 2015;51:935–43.
[3] Tlsty TD, Coussens LM. Tumor stroma and regulation of cancer development. Annu Rev Pathol 2006;1:119–50.
[4] Kalluri R, Zeisberg M. Fibroblasts in cancer. Nat Rev Cancer 2006;6:392–401.
[5] Liu M, Casimiro MC, Wang C, Shirley LA, Jiao X, Katiyar S, et al. p21CIP1 attenuates Ras- and c-Myc-dependent breast tumor epithelial mesenchymal transition and cancer stem cell-like gene expression in vivo. Proc Natl Acad Sci U S A 2009;106:19035–9.
[6] Cirri P, Chiarugi P. Cancer associated fibroblasts: the dark side of the coin. Am J Cancer Res 2011;1:482–97.
[7] Lee TH, D'Asti E, Magnus N, Al-Nedawi K, Meehan B, Rak J. Microvesicles as mediators of intercellular communication in cancer–the emerging science of cellular 'debris'. Semin Immunopathol 2011;33:455–67.
[8] Yang F, Ning Z, Ma L, Liu W, Shao C, Shu Y, et al. Exosomal miRNAs and miRNA dysregulation in cancer-associated fibroblasts. Mol Cancer 2017;16:148.
[9] Simons M, Raposo G. Exosomes–vesicular carriers for intercellular communication. Curr Opin Cell Biol 2009;21:575–81.
[10] Cocucci E, Racchetti G, Meldolesi J. Shedding microvesicles: artefacts no more. Trends Cell Biol 2009;19:43–51.
[11] Syn N, Wang L, Sethi G, Thiery JP, Goh BC. Exosome-Mediated Metastasis: from Epithelial-Mesenchymal transition to Escape from Immunosurveillance. Trends Pharmacol Sci 2016;37:606–17.
[12] Chen L, Guo P, He Y, Chen Z, Chen L, Luo Y, et al. HCC-derived exosomes elicit HCC progression and recurrence by epithelial-mesenchymal transition through MAPK/ERK signalling pathway. Cell Death Dis 2018;9:513.
[13] Yang WW, Yang LQ, Zhao F, Chen CW, Xu LH, Fu J, et al. Epiregulin Promotes Lung Metastasis of Salivary Adenoid Cystic Carcinoma. Theranostics 2017;7:3700–14.
[14] He L, Hannon GJ. MicroRNAs: small RNAs with a big role in gene regulation. Nat Rev Genet 2004;5:522–31.
[15] Calin GA, Croce CM. Chromosomal rearrangements and microRNAs: a new cancer link with clinical implications. J Clin Invest 2007;117:2059–66.
[16] Zhang L, Huang J, Yang N, Greshock J, Megraw MS, Giannakakis A, et al. microRNAs exhibit high frequency genomic alterations in human cancer. Proc Natl Acad Sci U S A 2006;103:9136–41.
[17] Chou J, Werb Z. MicroRNAs play a big role in regulating ovarian cancer-associated fibroblasts and the tumor microenvironment. Cancer Discov 2012;2:1078–80.
[18] Bovy N, Blomme B, Freres P, Dederen S, Nivelles O, Lion M, et al. Endothelial exosomes contribute to the antitumor response during breast cancer neoadjuvant chemotherapy via microRNA transfer. Oncotarget 2015;6:10253–66.
[19] Li YY, Zhou CX, Gao Y. Interaction between oral squamous cell carcinoma cells and fibroblasts through TGF-beta1 mediated by podoplanin. Exp Cell Res 2018;369:43–53.
[20] Thery C, Amigorena S, Raposo G, Clayton A. Isolation and characterization of exosomes from cell culture supernatants and biological fluids. Curr Protoc Cell Biol 2006; Chapter 3: Unit 3 22.
[21] Cheung LW, Leung PC, Wong AS. Gonadotropin-releasing hormone promotes ovarian cancer cell invasiveness through c-Jun NH2-terminal kinase-mediated activation of matrix metalloproteinase (MMP)-2 and MMP-9. Cancer Res 2006;66:10902–10.
[22] Cao ZG, Huang YN, Yao L, Liu YR, Hu X, Hou YF, et al. Positive expression of miR-361-5p indicates better prognosis for breast cancer patients. J Thorac Dis 2016;8:1772–9.
[23] Liu H, Chen W, Zhi X, Chen EJ, Wei T, Zhang J, et al. Tumor-derived exosomes promote tumor self-seeding in hepatocellular carcinoma by transferring miRNA-25-5p to enhance cell motility. Oncogene 2018;37:4964–78.
[24] Hashimoto K, Ochi H, Sunamura S, Kosaka N, Mabuchi Y, Fukuda T, et al. Cancer-secreted hsa-miR-940 induces an osteoblastic phenotype in the bone metastatic microenvironment via targeting ARHGAP1 and FAM134A. Proc Natl Acad Sci U S A 2018;115:2204–9.
[25] Gao J, Li N, Dong Y, Li S, Xu L, Li X, et al. miR-34a-5p suppresses colorectal cancer metastasis and predicts recurrence in patients with stage II/III colorectal cancer. Oncogene 2015;34:4142–52.
[26] Pu Y, Zhao F, Wang H, Cai S. MiR-34a-5p promotes multi-chemoresistance of osteosarcoma through down-regulation of the DLL1 gene. Sci Rep 2017;7:44218.
[27] Brand TM, Iida M, Stein AP, Corrigan KL, Braverman CM, Coan JP, et al. AXL is a Logical Molecular Target in Head and Neck Squamous Cell Carcinoma. Clin Cancer Res 2015;21:2601–12.
[28] Cichon MA, Szentpetery Z, Caley MP, Papadakis ES, Mackenzie IC, Brennan CH, et al. The receptor tyrosine kinase Axl regulates cell-cell adhesion and stemness in cutaneous squamous cell carcinoma. Oncogene 2014;33:4185–92.
[29] Medici D, Hay ED, Olsen BR. Snail and Slug promote epithelial-mesenchymal transition through beta-catenin-T-cell factor-4-dependent expression of transforming growth factor-beta3. Mol Biol Cell 2008;19:4875–87.
[30] Rana S, Malinowska K, Zoller M. Exosomal tumor microRNA modulates premetastatic organ cells. Neoplasia 2013;15:281–95.
[31] De Wever O, Demetter P, Mareel M, Bracke M. Stromal myofibroblasts are drivers of invasive cancer growth. Int J Cancer 2008;123:2229–38.
[32] Gao MQ, Kim BG, Kang S, Choi YP, Yoon JH, Cho NH. Human breast cancer-associated fibroblasts enhance cancer cell proliferation through increased TGF-alpha cleavage by ADAM17. Cancer Lett 2013;336:240–6.
[33] Abulaiti A, Shintani Y, Funaki S, Nakagiri T, Inoue M, Sawabata N, et al. Interaction between non-small-cell lung cancer cells and fibroblasts via enhancement of TGF-beta signaling by IL-6. Lung Cancer 2013;82:204–13.
[34] Marsh D, Dickinson S, Neill GW, Marshall JF, Hart IR, Thomas GJ. Alpha vbeta 6 Integrin promotes the invasion of morphoeic basal cell carcinoma through stromal modulation. Cancer Res 2008;68:3295–303.
[35] Cai J, Tang H, Xu L, Wang X, Yang C, Ruan S, et al. Fibroblasts in omentum activated by tumor cells promote ovarian cancer growth, adhesion and invasiveness. Carcinogenesis 2012;33:20–9.
[36] Fullar A, Kovalszky I, Bitsche M, Romani A, Schartinger VH, Sprinzl GM, et al. Tumor cell and carcinoma-associated fibroblast interaction regulates matrix metalloproteinases and their inhibitors in oral squamous cell carcinoma. Exp Cell Res 2012;318:1517–27.
[37] Stuelten CH, Dacosta Byfield S, Arany PR, Karpova TS, Stetler-Stevenson WG, Roberts AB. Breast cancer cells induce stromal fibroblasts to express MMP-9 via secretion of TNF-alpha and TGF-beta. J Cell Sci 2005;118:2143–53.
[38] Hannafon BN, Ding WQ. Intercellular communication by exosome-derived microRNAs in cancer. Int J Mol Sci 2013;14:14240–69.
[39] Tkach M, Thery C. Communication by Extracellular Vesicles: where we are and where we need to go. Cell 2016;164:1226–32.
[40] Vader P, Breakefield XO, Wood MJ. Extracellular vesicles: emerging targets for cancer therapy. Trends Mol Med 2014;20:385–93.
[41] Singh R, Pochampally R, Watabe K, Lu Z, Mo YY. Exosome-mediated transfer of miR-10b promotes cell invasion in breast cancer. Mol Cancer 2014;13:256.
[42] Fabbri M, Paone A, Calore F, Galli R, Gaudio E, Santhanam R, et al. MicroRNAs bind to Toll-like receptors to induce prometastatic inflammatory response. Proc Natl Acad Sci U S A 2012;109:E2110–6.
[43] Zhang Z, Li X, Sun W, Yue S, Yang J, Li J, et al. Loss of exosomal miR-320a from cancer-associated fibroblasts contributes to HCC proliferation and metastasis. Cancer Lett 2017;397:33–42.
[44] Pu Y, Zhao F, Li Y, Cui M, Wang H, Meng X, et al. The miR-34a-5p promotes the multi-chemoresistance of osteosarcoma via repression of the AGTR1 gene. BMC Cancer 2017;17:45.
[45] O'Bryan JP, Frye RA, Cogswell PC, Neubauer A, Kitch B, Prokop C, et al. Axl, a transforming gene isolated from primary human myeloid leukemia cells, encodes a novel receptor tyrosine kinase. Mol Cell Biol 1991;11:5016–31.
[46] Li Y, Ye X, Tan C, Hongo JA, Zha J, Liu J, et al. Axl as a potential therapeutic target in cancer: role of Axl in tumor growth, metastasis and angiogenesis. Oncogene 2009;28:3442–55.

[47] Graham DK, Deryckere D, Davies KD, Earp HS. The TAM family: phosphatidylserine sensing receptor tyrosine kinases gone awry in cancer. Nat Rev Cancer 2014;14:769–85.
[48] Krisanaprakornkit S, Iamaroon A. Epithelial-mesenchymal transition in oral squamous cell carcinoma. ISRN Oncol 2012; 2012: 681469.
[49] Linger RM, Keating AK, Earp HS, Graham DK. TAM receptor tyrosine kinases: biologic functions, signaling, and potential therapeutic targeting in human cancer. Adv Cancer Res 2008;100:35–83.
[50] Asiedu MK, Beauchamp-Perez FD, Ingle JN, Behrens MD, Radisky DC, Knutson KL. AXL induces epithelial-to-mesenchymal transition and regulates the function of breast cancer stem cells. Oncogene 2014;33:1316–24.
[51] Li YY, Zhou CX, Gao Y. Snail regulates the motility of oral cancer cells via RhoA/Cdc42/p-ERM pathway. Biochem Biophys Res Commun 2014;452:490–6.
[52] Miyoshi A, Kitajima Y, Kido S, Shimonishi T, Matsuyama S, Kitahara K, et al. Snail accelerates cancer invasion by upregulating MMP expression and is associated with poor prognosis of hepatocellular carcinoma. Br J Cancer 2005;92:252–8.
[53] Beach S, Tang H, Park S, Dhillon AS, Keller ET, Kolch W, et al. Snail is a repressor of RKIP transcription in metastatic prostate cancer cells. Oncogene 2008;27:2243–8.
[54] Miyoshi A, Kitajima Y, Sumi K, Sato K, Hagiwara A, Koga Y, et al. Snail and SIP1 increase cancer invasion by upregulating MMP family in hepatocellular carcinoma cells. Br J Cancer 2004;90:1265–73.